Biexciton states and two-photon absorption in molecular monolayers

Francis C. Spano
Department of Chemistry, Temple University, Philadelphia, Pennsylvania 19122
Vladimir Agranovich
Institute of Spectroscopy, USSR Academy of Sciences, Troitsk, Moscow Region 142092, USSR
Shaul Mukamel
Department of Chemistry, University of Rochester, Rochester, New York 14627

(Received 4 February 1991; accepted 9 April 1991)

Exciton–exciton interactions in doubly electronically excited molecular monolayers, may result in the formation of bound two-exciton states (biexcitons), whose binding is induced by the change in the molecular permanent dipole moments upon electronic excitation. We solve for the biexciton energies in the dipole approximation, and explore the effects of biexcitons on the monolayer nonlinear susceptibility. Calculations are made for monolayers with molecular dipole moments oriented either parallel or perpendicular to the monolayer surface.

I. INTRODUCTION

There is currently a great interest in the nonlinear optical properties of geometrically confined excitonic systems such as semiconductor quantum dots, wires, and wells,[1–3] and molecular aggregates[4–6] and monolayers.[7,8] The effects of sample size and shape on the excitonic resonances, lifetimes, and nonlinear optical response, provide an invaluable insight on the way bulk crystal properties evolve from single atomic or molecular properties. In addition, a microscopic understanding of the optical properties of geometrically restricted systems is important for the fabrication of nanostructure optical devices. Dramatic effects of reduced dimensionality have been observed in semiconductors. The increased binding energy of Wannier excitons in quantum wells leads to a greater stability and consequently, an increased nonlinear optical response,[2] even at room temperature where normally bulk excitons are not observed. Blue spectral shifts due to quantum confinement of Wannier excitons have been measured in semiconductor quantum dots such as CdS microcrystallites.[3] Size effects have also been reported in molecular aggregates. For example, size-dependent spectral shifts and radiative decay rates occur in aggregated dye molecules such as cyanine dyes.[4–6]

Molecular monolayers made by either Langmuir–Blodgett or self-assembly methods[7,8] provide an ideal system for studying the effects of reduced dimensionality. Very recently, molecular beam epitaxial methods have been successfully applied for growing molecular multilayers.[9] Monolayers of dye molecules with donor-acceptor substituents, whose excited state involves an intramolecular charge transfer, are particularly interesting for nonlinear optical applications.[8] These systems are characterized by a large change in the permanent dipole moment upon optical excitation. The goal of the present work is to study theoretically the elementary electronic excitations in molecular monolayers.

The linear optical properties of a molecular monolayer may usually be interpreted using a noninteracting (boson) picture of the elementary excitations, the Frenkel excitons.[10–12] However, in order to calculate correctly the nonlinear optical response, we need to go beyond the noninteracting Frenkel exciton model, and consider the effects of exciton–exciton scattering due to the Pauli exclusion principle, as well as attractive exciton–exciton interactions, which may lead to the formation of bound two-exciton states, denoted biexcitons, and other exciton complexes (triexcitons, etc.). These new types of elementary excitations may strongly affect the frequency dependent nonlinear susceptibilities, and should be properly taken into account. The calculation of optical susceptibilities requires the carrying out of a summation over all virtual excited states. Far from excitonic resonances, the main contribution to $\chi^{(3)}$ comes from single-exciton virtual states (for molecular crystals these states correspond to Frenkel excitons or charge transfer excitons). However, for frequencies ω which are close to the excitonic transition frequency ω_s, the frequency 2ω will be close to the frequency of two-particle states $2\omega \sim 2\omega_s$. In this case, taking into account exciton–exciton interactions is essential. It may result in the formation of biexcitons and consequently give new types of resonances. The exciton–exciton interaction was used by Toshich[13] for the calculation of nonlinear susceptibilities. Its origin, related to the excited electronic state permanent dipole moments, was discussed in detail by Fox.[14]

The nonlinear optical response of a one dimensional array of nonpolar molecules was recently calculated by Spano and Mukamel.[15] The effects of exciton–exciton scattering due to the Pauli exclusion principle (with no binding potential and hence no biexciton formation) were studied in detail. It was shown that the third order nonlinear hyperpolarizability of a molecular aggregate, may indeed be enhanced by a factor of N, and scale as $\sim N^2$ when the aggregate length Na is much smaller than an optical wavelength. Here, N is the number of molecules in the aggregate and a is the near neighbor intermolecular spacing. This enhancement also requires that the superradiant damping of the excited electronic state $N\gamma$ be quenched by a rapid homogeneous dephasing. (γ is the radiative decay rate of a single molecule.) However, as the aggregate length increases to values well beyond an optical wavelength, the enhancement levels off. A cancellation between excitonic nonlinearities and exciton–two-exciton nonlinearities prevents a coherent enhancement for molecules separated by more than an optical wavelength. A mapping of the system to coupled anharmonic

0021-9606/91/141400-10$03.00

oscillators[15(b)] provides a simple physical picture. Ishihara and Cho[16] have calculated the third order response for a general combination of external field wave vectors. Their calculation, which neglected radiative damping, also showed that the cooperative enhancement levels off for large N. We expect the exciton–exciton scattered states in the two-exciton continuum of an infinite two-dimensional plane to behave in a similar fashion, i.e., the enhancement of the nonlinear optical response should be determined by the number of molecules within a square optical wavelength $(\lambda/a)^2$. However, the possible existence of biexciton states, may lead to a resonance enhanced nonlinear response outside the two-exciton continuum.

The theory of biexcitons closely parallels that of biphonons (bound states of two optical phonons), which were studied in considerable detail.[17] The anharmonic nonlinear interaction of biphonons arises from the fact that the energy of a double vibrational excitation of a single molecule is less than twice the single vibrational energy. Agranovich and coworkers[17] and Efremov and Kaminskaya[18] predicted that the existence of biphonon states should lead to new resonances in the second and third order nonlinear susceptibilities. Efremov and Kozhushner and Efremov and Kaminskaya[19] later showed the existence of biexcitons in a crystal with a general *isotropic* binding potential, and calculated the biexciton dispersion curve for a cubic molecular crystal.

In this work we develop a theory for the biexciton energy, and the transition dipole moment from the single-exciton state, in a molecular monolayer with Frenkel excitons, and use these quantities to calculate two-photon absorption (TPA), which is a common spectroscopic technique related to the third order nonlinear response $\chi^{(3)}$. The effects of the Pauli exclusion principle are treated exactly. Single excitons coupled to the electromagnetic field, i.e., polaritons, in two dimensions have been investigated by Agranovich and Dubovski[20] and Philpott and Sherman[21] and others.[22,23] In these works one of the two polariton branches was found to be superradiant; the radiative lifetime is $(\lambda/a)^2$ times shorter than the lifetime of a single molecule.[20] The present work treats the optical properties of Coulombic biexcitons in two dimensions. We do not consider the more general problem of biexciton polaritons.[23]

In Sec. II, the model Hamiltonian for a square lattice of two-level molecules which interact via transition and permanent dipole–dipole coupling, is presented. In Sec. III, the method by which biexcitons are calculated is developed. In the following section, biexciton dispersion curves, along with the transition dipole strengths are calculated for molecular dipole moments oriented either parallel or perpendicular to the monolayer surface. In dye aggregates these geometries are referred to as J aggregates and H aggregates, respectively.[4–6] The nearest neighbor transition dipole–dipole coupling is negative in the former and positive in the latter geometries. The two-photon absorption is discussed in Sec. V, and our results are summarized in the final section.

II. MODEL HAMILTONIAN

We consider a two-dimensional square lattice with N^2 two-level molecules, each having a ground and an excited electronic state with transition dipole moment $\boldsymbol{\mu}$ and gas phase electronic transition frequency ω_0'. In addition, the ground and excited states have permanent dipole moments denoted $\boldsymbol{\mu}^g$ and $\boldsymbol{\mu}^f$, respectively. The effective system Hamiltonian, including transition and permanent dipole–dipole interactions is derived in Appendix A [Eq. (A9)]. In the present work we retain only the terms which conserve the number of excitons,

$$H=\omega_0\sum_{\mathbf{n}} b^\dagger_{\mathbf{n}} b_{\mathbf{n}}+\sum_{\mathbf{m},\mathbf{n}} V(\mathbf{m}-\mathbf{n}) b^\dagger_{\mathbf{m}} b_{\mathbf{n}} + \sum_{\mathbf{m},\mathbf{n}} A(\mathbf{m}-\mathbf{n}) b^\dagger_{\mathbf{m}} b^\dagger_{\mathbf{n}} b_{\mathbf{m}} b_{\mathbf{n}}. \tag{2.1}$$

In Eq. (2.1) a factor of $\hbar$ is omitted so that energy is in units of s^{-1}. The summations are over the entire lattice, i.e., $m_x, m_y = -(N-1)a/2,\dots,(N-1)a/2$. (Throughout this article we take N to be odd, this should have no effect on our results since N will eventually be taken to infinity.) We assume cyclic boundary conditions so that $\mathbf{m}+N\mathbf{x}=\mathbf{m}$, and $\mathbf{m}+N\mathbf{y}=\mathbf{m}$, where $\mathbf{x}$ and $\mathbf{y}$ are the square lattice vectors, $\mathbf{x}=a\mathbf{i}$ and $\mathbf{y}=a\mathbf{j}$, where $\mathbf{i}$ and $\mathbf{j}$ are unit vectors and a is the lattice spacing. $b^\dagger_n$ and b_n are the creation and annihilation operators, respectively, for electronic excitation at site $\mathbf{n}$, obeying Fermi anticommutation relations when both operators correspond to the same site,

$$[b^\dagger_n, b_m]_+ = \delta_{mn} + (1-\delta_{mn}) 2 b^\dagger_n b_m$$

and

$$[b_n, b_m]_+ = (1-\delta_{mn}) 2 b_n b_m. \tag{2.2}$$

In Eq. (2.1) we have omitted a constant term E_g which in our approximation is the permanent dipole interaction energy when all molecules are unexcited, and is given by $E_g=\frac{1}{2}\Sigma_{\mathbf{m},\mathbf{n}}\,\mu^g_{\mathbf{m}} \mathsf{T}_{\mathbf{mn}} \mu^g_{\mathbf{n}}$. The near-field dipole–dipole interaction tensor is given by $T_{mn}=(r^2-3\mathbf{rr})/r^5$, where $\mathbf{r}=\mathbf{m}-\mathbf{n}$. The monolayer transition frequency is renormalized to the value ω_0 by the interaction of a single excited state permanent dipole moment with the remaining ground state permanent dipoles, and is equal to [see Eq. (A.3)]

$$\omega_0 \equiv \omega_0' + \sum_{\mathbf{m},\mathbf{n}} \Delta\boldsymbol{\mu}_{\mathbf{m}} \mathsf{T}_{\mathbf{mn}} \boldsymbol{\mu}^g_{\mathbf{n}}, \tag{2.3}$$

with the change in dipole moment given by $\Delta\boldsymbol{\mu} \equiv \boldsymbol{\mu}^f - \boldsymbol{\mu}^g$. The second term in Eq. (2.1) represents the coupling between transition dipole moments at sites $\mathbf{m}$ and $\mathbf{n}$ with [see Eq. (A.8)]. $V(\mathbf{m}-\mathbf{n})$ is given by

$$V(\mathbf{m}-\mathbf{n}) = \boldsymbol{\mu}_m \mathsf{T}_{mn} \boldsymbol{\mu}_n. \tag{2.4}$$

The last term in Eq. (2.1) represents exciton–exciton interaction, and $A(\mathbf{m}-\mathbf{n})$ is given by

$$A(\mathbf{m}-\mathbf{n}) = \tfrac{1}{2}\Delta\boldsymbol{\mu}_m \mathsf{T}_{mn} \Delta\boldsymbol{\mu}_n. \tag{2.5}$$

In the present article, we further invoke a nearest neighbor approximation for the transition dipole coupling and the permanent dipole interaction, resulting in

$$V(\mathbf{m}-\mathbf{n}) = V_x \delta_{m_y,n_y} \delta_{m_x,n_x\pm a} + V_y \delta_{m_x,n_x} \delta_{m_y,n_y\pm a} \tag{2.6}$$

and

$$A(\mathbf{m}-\mathbf{n}) = A_x \delta_{m_y,n_y} \delta_{m_x,n_x\pm a} + A_y \delta_{m_x,n_x} \delta_{m_y,n_y\pm a}. \tag{2.7}$$

III. COULOMBIC EXCITONS AND BIEXCITONS

When polariton effects are neglected, a weak electromagnetic wave of wave vector **k**, interacting with a molecular monolayer, creates Coulombic excitons of wave vector κ, where κ is the tangential component of **k** in the monolayer plane. Using the localized site basis $|\mathbf{n}\rangle$, where $|\mathbf{n}\rangle \equiv b_{\mathbf{n}}^{\dagger}|0\rangle$ and $|0\rangle$ is the ground state with all molecules unexcited, the excitonic wave function is given by

$$\varphi(\kappa) \equiv \frac{1}{N} \sum_{\mathbf{m}} e^{i\kappa \cdot \mathbf{m}} |\mathbf{m}\rangle. \qquad (3.1)$$

$\phi(\kappa)$ in Eq. (3.1) is an eigenstate of the Hamiltonian Eq. (2.1), with energy

$$\omega(\kappa) \equiv \omega_0 + \sum_{\mathbf{m}} V(\mathbf{m}) e^{i\kappa \cdot \mathbf{m}}, \qquad (3.2)$$

and cyclic boundary conditions ($|\mathbf{m}\rangle = |\mathbf{m} + N\mathbf{x}\rangle = |\mathbf{m} + N\mathbf{y}\rangle$) require that $\kappa_x, \kappa_y = 2\pi n/Na$ with $n = 0,1,\ldots N-1$. Making use of Eq. (2.6), Eq. (3.2) becomes

$$\omega(\kappa) \equiv \omega_0 + 2V_x \cos(\kappa \cdot \mathbf{x}) + 2V_y \cos(\kappa \cdot \mathbf{y}). \qquad (3.3)$$

The calculation of the doubly excited wave functions is more complicated because two excitations cannot reside on a single site (Pauli exclusion principle), and because of the exciton–exciton interaction $A(\mathbf{m} - \mathbf{n})$. We calculate the biexciton states by generalizing a procedure originally developed by Wortis[24] in treating bimagnon states in the Heisenberg ferromagnet, to include an arbitrary form of $A(\mathbf{m} - \mathbf{n})$. We begin by writing a general translationally invariant two-exciton wave function,

$$\Psi(\mathbf{K}) \equiv \frac{1}{N} \sum_{\mathbf{R}} \sum_{\mathbf{r}}{}' e^{i\mathbf{K} \cdot \mathbf{R}} \psi_{\mathbf{K}}(\mathbf{r}) b_{\mathbf{R} - (r/2)}^{\dagger} b_{\mathbf{R} + (r/2)}^{\dagger} |0\rangle. \qquad (3.4)$$

K is the momentum conjugate to the center of mass coordinate **R** for a pair of excitations separated by **r**. The periodic boundary conditions result in a wave function which is invariant when $\mathbf{R} \equiv (\mathbf{m} + \mathbf{n})/2$ is replaced by $\mathbf{R} + N\mathbf{x}/2$ or $\mathbf{R} + N\mathbf{y}/2$. This yields the following allowed values of K: $K_x, K_y = 4\pi n/Na$, $n = 0,1,\ldots N-1$. The summation prime in Eq. (3.4) indicates that $-\mathbf{r}$ and $\mathbf{0}$ are excluded since, by symmetry, $\psi(\mathbf{r}) = \psi(-\mathbf{r})$ and because $\psi(\mathbf{0})$ is not allowed by the exclusion principle. $\psi(\mathbf{r})$ is normalized so that

$$\sum_{\mathbf{r}}{}' |\psi_{\mathbf{K}}(\mathbf{r})|^2 = 1. \qquad (3.5)$$

Substituting $\Psi(\mathbf{K})$ into the Schrödinger equation, $H\Psi(\mathbf{K}) = E\Psi(\mathbf{K})$, we obtain an equation for $\psi_K(\mathbf{r})$

$$(E - 2\omega_0)\psi_{\mathbf{K}}(\mathbf{r}) - 2\sum_{\delta'} V(\delta')\cos\left(\frac{\mathbf{K}}{2}\boldsymbol{\delta}'\right)\psi_{\mathbf{K}}(\mathbf{r} + \boldsymbol{\delta}')$$
$$= 2A(\mathbf{r})\psi_{\mathbf{K}}(\mathbf{r}) - 2V(\mathbf{r})\cos\left(\frac{\mathbf{K}}{2}\mathbf{r}\right)\psi_{\mathbf{K}}(0), \qquad (3.6)$$

where, $\boldsymbol{\delta}' = \mathbf{x}, -\mathbf{x}, \mathbf{y}$ or $-\mathbf{y}$. $\psi_{\mathbf{K}}(0)$ is not an admissible component of the wave function since two excitations cannot reside on the same site; only Eq. (3.6) with $\mathbf{r} \neq 0$ follows from the Schrödinger equation. However, since the wave function for values of $\mathbf{r} \neq 0$ is not coupled to the $\mathbf{r} = 0$ value (the term with $\mathbf{r} = 0$ on the right-hand side is canceled by one on the left-hand side) it proves convenient to retain the $r = 0$ component, which is then *defined* by Eq. (3.6), and rewrite Eq. (3.6) in momentum space,

$$f_{\mathbf{K}}(\mathbf{q}) \equiv \frac{1}{N} \sum_{\mathbf{r}} e^{i\mathbf{q} \cdot \mathbf{r}} \psi_{\mathbf{K}}(\mathbf{r}), \qquad (3.7)$$

where the summation over **r** is now $r_x, r_y = -(N-1)a/2,\ldots,(N-1)a/2$, including $r_x = r_y = 0$. Periodic boundary conditions allow the following values of **q**: $q_x, q_y = 2\pi n/Na, n = 0,1,\ldots N-1$. Equation (3.6) is now transformed to

$$f_{\mathbf{K}}(\mathbf{q}) = \sum_{\mathbf{q}'} \frac{2N^{-2} \Sigma_{\delta'} \cos(\mathbf{q} \cdot \boldsymbol{\delta}')\{A(\boldsymbol{\delta}')\cos(\mathbf{q}' \cdot \boldsymbol{\delta}') - V(\boldsymbol{\delta}')\cos[(\mathbf{K}/2) \cdot \boldsymbol{\delta}']\}}{E - \Omega(\mathbf{K},\mathbf{q})} f_{\mathbf{K}}(\mathbf{q}'), \qquad (3.8)$$

where the energy of two free excitons with wave vectors $\mathbf{K}/2 + \mathbf{q}$ and $\mathbf{K}/2 - \mathbf{q}$ is given by

$$\Omega(\mathbf{K},\mathbf{q}) \equiv 2\omega_0 + 4\sum_{\delta} V_{\delta} \cos\left(\frac{\mathbf{K}}{2} \cdot \boldsymbol{\delta}\right)\cos(\mathbf{q} \cdot \boldsymbol{\delta}), \qquad (3.9)$$

with $\delta = \mathbf{x}$ or $\mathbf{y}$. Finally, Eq. (3.8) can be written as a vector 2×2 matrix equation,

$$U_{\gamma}(\mathbf{K}) = \sum_{\delta} M_{\gamma,\delta}(\mathbf{K},E) U_{\delta}(\mathbf{K}), \qquad (3.10)$$

with the two-component vector $U_{\gamma}(\mathbf{K}), \gamma = x,y$, defined by

$$U_{\gamma}(\mathbf{K}) \equiv \sum_{\mathbf{q}} \left\{V_{\gamma} \cos\left(\frac{\mathbf{K}}{2} \cdot \gamma\right) - A_{\gamma} \cos(\mathbf{q} \cdot \gamma)\right\} f_{\mathbf{K}}(\mathbf{q}), \qquad (3.11)$$

and the 2×2 matrix

$$M_{\gamma\delta}(\mathbf{K},E) \equiv 4N^{-2} \sum_{\mathbf{q}} \frac{\{A_{\gamma} \cos(\mathbf{q} \cdot \boldsymbol{\gamma}) - V_{\gamma} \cos[(\mathbf{K}/2) \cdot \boldsymbol{\gamma}]\}\cos(\mathbf{q} \cdot \boldsymbol{\delta})}{E - \Omega(\mathbf{K},\mathbf{q})}. \qquad (3.12)$$

When N is taken to infinity, we replace the sum by an integral, resulting in,

$$M_{\gamma\delta}(\mathbf{K},E) = \frac{4a^2}{\pi^2} \int_0^{\pi/a} \int_0^{\pi/a} dq_x\, dq_y \frac{\{A_{\gamma} \cos(q_{\gamma}a) - V_{\gamma} \cos(K_{\gamma}a/2)\}\cos(q_{\delta}a)}{E - \Omega(\mathbf{K},\mathbf{q})}. \qquad (3.13)$$

The integrals in Eq. (3.13) can be expressed as elliptic integrals of the first, second, and third kind, as described in detail in Ref. 24, and subsequently evaluated using standard numerical packages.

The eigenvalues E of Eq. (3.6) are obtained by solving the characteristic equation

$$\det[1-\mathsf{M}(\mathbf{K},E)]=0, \tag{3.14}$$

where 1 is the 2×2 identity matrix. This equation was solved for E by numerical iteration for each value of $\mathbf{K}$, resulting in the biexciton energies $E_b(\mathbf{K})$. The resulting eigenvalues E are then used to solve the 2×2 matrix equation (3.10) for the vector $U(\mathbf{K})$ up to an arbitrary constant which is later determined by the normalization condition. Finally, the wave function $\psi_{\mathbf{K}}(\mathbf{r})$ is given by

$$\psi_K(r)=\sum_{\delta} G_{r,\delta}[\mathbf{K};E_b(\mathbf{K})]\,U_\delta(\mathbf{K}), \tag{3.15}$$

where the Green function $G_{\mathbf{r},\mathbf{r}'}(\mathbf{K};E)$ is given by

$$G_{\mathbf{r},\mathbf{r}'}(\mathbf{K};E)=(4/N^2)\sum_{\mathbf{q}}\frac{\cos(\mathbf{q}\cdot\mathbf{r})\cos(\mathbf{q}\cdot\mathbf{r}')}{E-\Omega(\mathbf{K},\mathbf{q})}, \tag{3.16}$$

which in the limit of large N, assumes the form

$$G_{\mathbf{r},\mathbf{r}'}(\mathbf{K};E)=(4a^2/\pi^2)\int_0^{\pi/a}dq_x\int_0^{\pi/a}dq_y \times\frac{\cos(\mathbf{q}\cdot\mathbf{r})\cos(\mathbf{q}\cdot\mathbf{r}')}{E-\Omega(\mathbf{K},\mathbf{q})}. \tag{3.17}$$

IV. BIEXCITONS STATES

A. Eigenstates and energies

We now explore the possible formation of biexciton states. To that end, we adopt a specific geometry. The transition and the permanent dipole moments can in general be oriented in any direction relative to the monolayer plane. In the calculations presented below we assume that the permanent dipole moments are parallel to the transition dipole moments. We further consider only the two extreme geometries where the dipoles are oriented either parallel or perpendicular to the monolayer surface. Adopting the notation commonly used for molecular aggregates,[4-6] we shall refer to these geometries as J and H monolayers, respectively.

For a J monolayer, the transition dipoles in the monolayer plane are assumed to be aligned along the y axis, and we have

$$V_x=-\frac{1}{2}V_y=\frac{\mu^2}{a^3}, \tag{4.1}$$

$$A_x=-\frac{1}{2}A_y=\frac{(\Delta\mu)^2}{2a^3}. \tag{4.2}$$

In an H monolayer, where the transition dipoles are oriented perpendicular to the monolayer plane, we have

$$V_x=V_y=\frac{\mu^2}{a^3}, \tag{4.3}$$

$$A_x=A_y=\frac{\Delta\mu^2}{2a^3}. \tag{4.4}$$

In Figs. 1 and 2 we show the biexciton energy dispersion curves along two directions in K space $(K_x,0)$ and $(0,K_y)$, for the J monolayer (Fig. 1) and the H monolayer (Fig. 2), for several values of the dimensionless parameter $\Theta\equiv A_x/V_x$. It should be noted that since our states are the Coulomb states, their energies and the transition dipole moments may be nonanalytical functions of wave vectors at small k. The curves were calculated numerically by searching for the roots of Eq. (3.14). The dimensionless energy shown in these figures is defined as $e_b(K)\equiv[E_b(K)-2\omega_0]/4V_x$. One fourth of the Brillouin zone for K is shown, since by symmetry $e_b(2\pi/a\pm K)=e_b(K)$. Because the dipole interactions are isotropic in the H monolayer, the dispersion curves along $(K_x,0)$ and $(0,K_y)$ are identical so that only a single curve need be displayed. In order to test the accuracy of our numerics we studied the analytically solvable case when $K_x=K_y\approx\pi/a$, so that $\cos(\mathbf{K}/2\cdot\delta)=0$ and the two-exciton bandwidth is therefore zero. Eq. (3.6) shows that

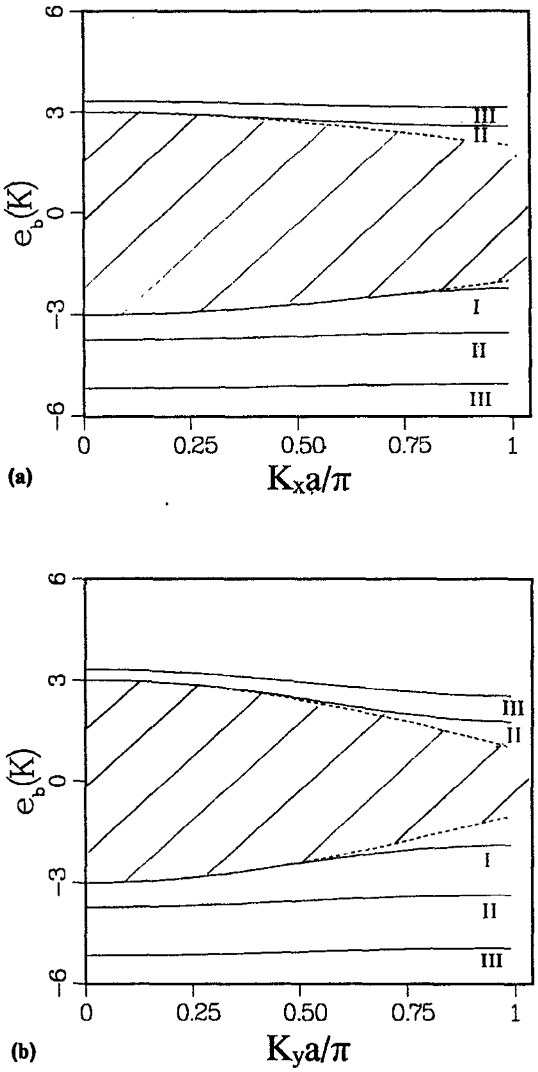

FIG. 1. (a) The biexciton dispersion curves for a J monolayer with $\Theta/\Theta_1'=1.1$ (I), 2 (II), and 3 (III), calculated numerically by solving Eq. (3.14). $K_y=0$ and K_x is varied. For $\Theta/\Theta_1'=1.1$ there is a single bound state. For $\Theta/\Theta_1'=2$ and 3, the second critical value of Θ is surpassed $(\Theta_2'/\Theta_1'\approx 1.6)$ and two bound states arise for all values of K_x, one above and one below the two exciton continuum, which is the shaded region. In (b) $K_x=0$ and K_y is varied.

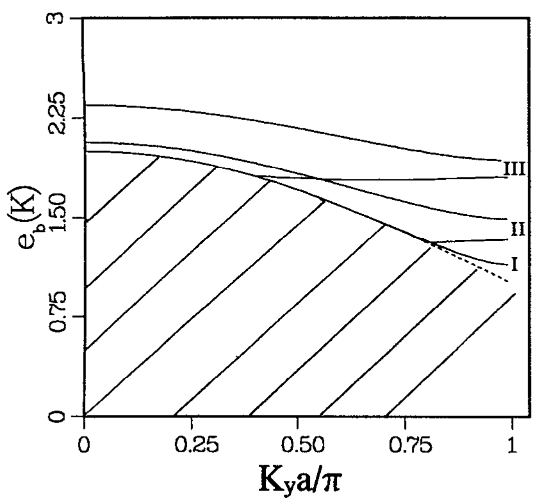

FIG. 2. The biexciton dispersion curves for an H monolayer with $\Theta/\Theta_1^H = 1.1$ (I), 2 (II), and 3 (III), calculated numerically by solving Eq. (3.14). $K_x = 0$ and K_y is varied. For $\Theta/\Theta_1^H = 1.1$ there is a single bound state. For $\Theta/\Theta_1^H = 2$ and 3, the second critical value of Θ is not surpassed ($\Theta_2^H/\Theta_1^H \approx 3.33$) so that, at $K = 0$, there is still only a single biexciton. However, for higher values of K the two-exciton bandwidth is smaller and hence the critical values are also smaller. For sufficiently high values of K two biexciton branches are observed.

the H-monolayer wave function is doubly degenerate with $e_b(K) = \Theta/2$, while the J monolayer has $e_b(K) = \Theta/2$ and $-\Theta$. These values were also obtained by our numerical procedure.

The most notable feature in Figs. 1 and 2 is the emergence of one or two bound states for each value of K, depending on the magnitude of Θ. In the J monolayer at $\mathbf{K} = 0$, a single bound state appears below the two-exciton continuum when Θ surpasses the critical value of $\Theta_1^J = 1.6$. Further increases in Θ above the second critical value $\Theta_2^J = 2.6$ result in a second bound state which is now located *above* the two-exciton continuum. In the H monolayer both bound states are above the two exciton continuum. For optical excitation at $\mathbf{K} = 0$, we have $\Theta_1^H = 1.1$ and $\Theta_2^H = 3.6$. For both J and H monolayers, the critical value decreases as the magnitude of K_x or K_y increases. The dispersion of biexciton states is negligible in comparison to the bandwidth of the exciton states. This is very similar to the behavior of biphonons.[17]

In Figs. 3 and 4 we show the $K = 0$, low energy J (below continuum), and high energy (higher of the two bound states when $\Theta > \Theta_2^H$) H-monolayer wave functions, respectively, as a function of the relative coordinate $\mathbf{r}$, calculated by using Eq. (3.15). The J-monolayer wave function is highly oscillatory and changes sign at every site in the x direction, but remains of like sign in the y direction. The H-monolayer wave function, however, has no nodes. For Θ near Θ_1^J and Θ_1^H the wave functions in both cases extend over many lattice sites. These properties can be directly deduced from Eq. (3.6); for the H monolayer with $\Theta \approx \Theta_1^H$ the biexciton energy is very close to the upper band edge, $E \approx 2\omega_0 + 8V_x$, so that when $r > 1$ Eq. (3.6) reduces to

$$8\psi_K(\mathbf{r}) - 2\psi_K(\mathbf{r}+\mathbf{x}) - 2\psi_K(\mathbf{r}-\mathbf{x}) - 2\psi_K(\mathbf{r}+\mathbf{y}) - 2\psi_K(\mathbf{r}-\mathbf{y}) \approx 0. \tag{4.5}$$

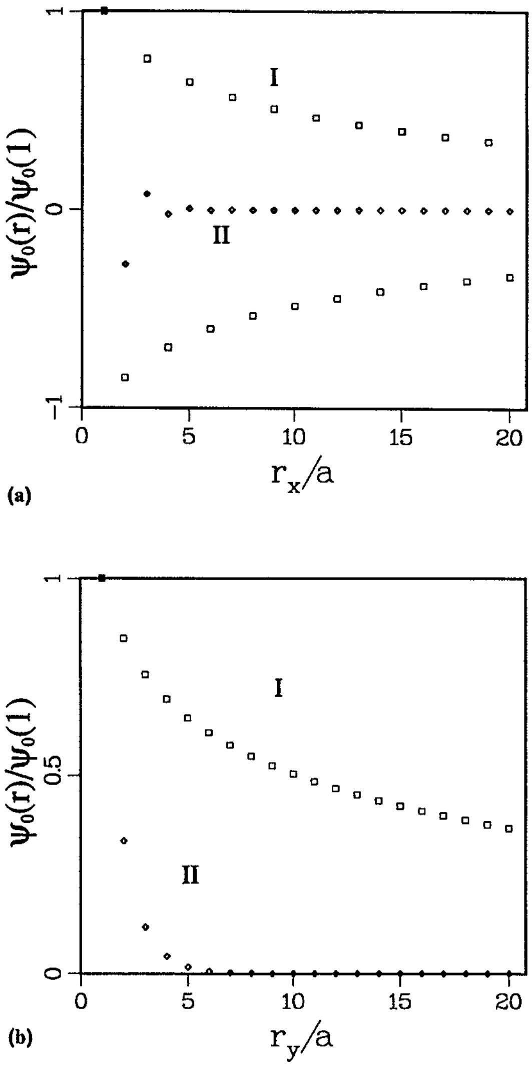

FIG. 3. (a) The normalized low energy $K = 0$ J-monolayer wave function as a function of x component of the relative coordinate r_x for $\Theta/\Theta_1^J = 1.1$ (I) and 2 (II), calculated numerically by first finding $E_b(0)$ from Eq. (3.14) and then using Eq. (3.15). In curve II, the wave function is highly localized, with an energy $e_b(0) = -3.7$, while in I it is largely delocalized with $e_b(0) \approx -3$. Localization increases as the eigenstate splits further off the continuum. *Note also the sign alternation as a function of* r_x. In (b) a different cross section of the same wave function is shown, $r_x = 0$ and r_y is varied. In this direction the oscillations disappear.

The last equation is satisfied by a slowly varying wave function, consistent with the one obtained numerically in Fig. 4. For the J-monolayer wave function with $\Theta \approx \Theta_1^J$ the same arguments lead to

$$-12\psi_K(\mathbf{r}) - 2\psi_K(\mathbf{r}+\mathbf{x}) - 2\psi_K(\mathbf{r}-\mathbf{x}) + 4\psi_K(\mathbf{r}+\mathbf{y}) + 4\psi_K(\mathbf{r}-\mathbf{y}) \approx 0, \tag{4.6}$$

which is satisfied by a wave function which changes little in magnitude but changes sign alternately in the x direction. For both monolayer types, as the binding energy Θ increases, the wave function becomes increasingly localized, and when Θ surpasses Θ_2 a new bound state emerges, above the two-exciton continuum. In the former case, when $\Theta \approx \Theta_2^J$ the new state above the continuum satisfies Eq. (4.6) but with the first term of opposite sign. It is easily seen that

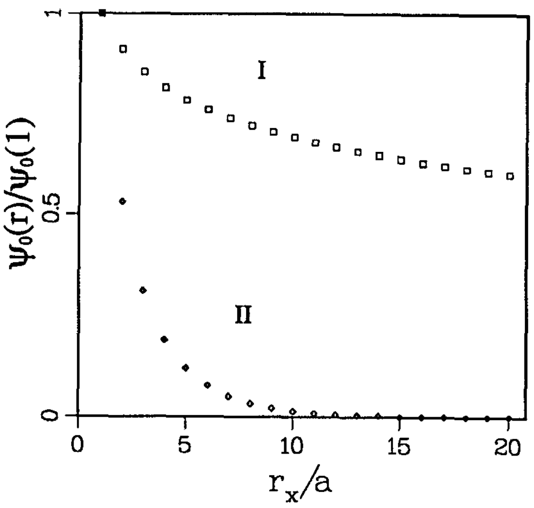

FIG. 4. The normalized low energy $K = 0$ H-monolayer wave function as a function of x component of the relative coordinate r_x for $\Theta/\Theta_1^H = 1.1$ (I) and 2 (II), calculated numerically by first finding $E_b(0)$ from Eq. (3.14) and then using Eq. (3.15). In curve II, the wave function is highly localized, with an energy $e_b(0) = 2.06$, while in I it is largely delocalized with $e_b(0) \approx 2.0$.

this state will therefore oscillate in sign along the y direction, opposite to its low energy partner. When Θ is very large ($\Theta > \sim 10$), the $K = 0$ biexciton collapses into a pair state along the y direction for the J monolayer and into a symmetrically distributed pair state in the x and y directions for the H monolayer.

B. Exciton–biexciton transition dipole moment

In order to calculate nonlinear optical properties and explore the possibility of new resonances outside the single-exciton and two-exciton continua, one needs to evaluate the transition dipole moments between the ground state and single exciton κ state, (we recall that κ is the component of the photon wave vector in the monolayer plane), and between the single exciton κ state to the biexciton 2κ state. This follows from the form of the radiation–matter interaction Hamiltonian, and the conservation law of wave vectors for quasiparticles.

It is easy to show,[23] that

$$\mu_{eb} \equiv \mu \langle \varphi(\kappa) | \sum_{\mathbf{m}} b_{\mathbf{m}} e^{-i\kappa\cdot\mathbf{m}} | \Psi(\mathbf{K}) \rangle. \tag{4.7}$$

Substitution of Eqs. (3.1) and (3.4) into Eq. (4.7) and performing the summations over **R** and **r** (which can be carried out independently), we get

$$\mu_{eb}(\mathbf{K}) = 2\mu\delta_{\mathbf{K},2\kappa} \sum_{\mathbf{r}}{}' \psi_{\mathbf{K}}(\mathbf{r}). \tag{4.8}$$

The summation prime indicates that $r_x = 0, 1a, 2a, \ldots, (N-1)a/2$ and $r_y = -(N-1)a/2, \ldots, (N-1)a/2$ excluding $r_x = r_y = 0$, i.e., the summation neglects $-\mathbf{r}$ and $\mathbf{0}$. A brute force evaluation of μ_{eb} involves numerically calculating $\phi_K(\mathbf{r})$ at each point $\mathbf{r}$ [by evaluating an integral like Eq. (3.12)] and summing over the lattice. A considerably simpler way, which involves the numerical evaluation of only a few integrals, is outlined in Appendix B. The final result is

$$\mu_{eb}(\mathbf{K}) = \mu\delta_{\mathbf{K},2\kappa} U_{\mathbf{x}}(\mathbf{K}) \left\{ \frac{1 + R(\mathbf{K})}{E_b(\mathbf{K}) - \Omega(\mathbf{K},0)} - G_{\mathbf{x},0}(\mathbf{K};E_b(\mathbf{K})) - R(\mathbf{K}) G_{y,0}(\mathbf{K};E_b(\mathbf{K})) \right\}, \tag{4.9a}$$

where

$$R(\mathbf{K}) \equiv [1 - M_{xx}(\mathbf{K},E_b)]/M_{xy}(\mathbf{K},E_b). \tag{4.9b}$$

The amplitudes $U_{\mathbf{x}}(\mathbf{K})$ are determined (up to a phase factor) by the wave function normalization condition and (see Appendix B) are given by

$$|U_{\mathbf{x}}(\mathbf{K})|^2 = 2\left(\frac{1}{\pi^2} \int_0^{\pi/a} dq_x \int_0^{\pi/a} dq_y \times \left\{ \frac{\cos(q_x a) + R(\mathbf{K})\cos(q_y a)}{E_b(\mathbf{K}) - \Omega(\mathbf{K},\mathbf{q})} \right\}^2 - \{ G_{\mathbf{x},0}(\mathbf{K},E_b(\mathbf{K})) + R(\mathbf{K}) G_{\mathbf{y},0}(\mathbf{K},E_b(\mathbf{K})) \}^2 \right)^{-1}. \tag{4.10}$$

Figure 5 displays $\log[\mu_{eb}^2(\mathbf{0})/\mu^2]$ as a function of Θ for the J monolayer and H monolayer. The calculations were made using Eq. (4.9) and Eq. (4.10). The two curves for the J monolayer correspond to the higher (above continuum) and lower (below continuum) energy biexciton states. Because $\mu_{eb}(\mathbf{K})$ is proportional to the integrated biexciton wave function, we find that the J monolayer near $K = 0$ has an extremely small exciton–biexciton transition dipole moment due to the wave function oscillations (see Fig. 3). As the

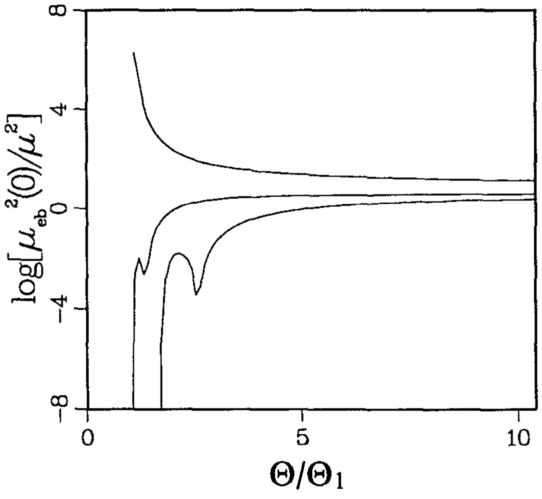

FIG. 5. The logarithm of $\mu_{eb}^2(0)/\mu^2$, as a function of Θ/Θ_1, where $\Theta_1 \equiv \Theta_1^H$ for the upper curve which corresponds to an H monolayer at $K = 0$, and $\Theta_1 \equiv \Theta_1^J$ for the two lower curves which correspond to the low energy (upper) and high energy (lower) J-monolayer biexcitons. The H-monolayer curve asymptotically approaches the value of $\log(8) = 0.9$, while the J-monolayer curves approach $\log(4) = 0.6$. These values follow from Eq. (4.10) and the limiting form of the wave function in both cases (see the text).

wave function becomes more localized (when Θ is increased), $\mu_{eb}^2(0)$ increases; in the limit of large Θ the $K=0$, biexciton is simply a pair state along the y direction and using Eq. (4.9), we have $\mu_{eb}^2(0)=2\mu^2$, which is what we obtain numerically as well. The high energy (above continuum) biexciton wave function also contains oscillations (along the y axis) and, consequently also initially has $\mu_{eb}^2(0) \ll \mu^2$. This is not the case for the H monolayer, however. At $K \approx 0$ the high energy, nodeless, biexciton states have dipole moments or orders of magnitude larger than μ. In this case the limiting value of $\mu_{eb}^2(0)$ is $\mu_{eb}^2(0)=8\mu^2$, since localization at $\mathbf{r}=\mathbf{x}$ and $\mathbf{r}=\mathbf{y}$ is equally probable. The low-energy partner, which is not shown, has a vanishing dipole moment at $K=0$ because this wave function is antisymmetric upon the interchange of the x and the y coordinates, i.e., there is a nodal line $x=y$.

V. NONLINEAR OPTICAL RESPONSE OF BIEXCITONS

In this section we explore the possibility of probing biexcitons using the third order nonlinear polarizability. To that end we consider only the part of the response that involves the biexciton states, and look for new two-photon resonances that are outside the two-exciton band. Note that in all our calculations of exciton and biexciton states, we took into account only Coulomb (instantaneous) interactions between charges, and retardation was neglected. This results in the Coulombic excitons and biexcitons.[25,26] We shall use these zero order states in the calculation of the nonlinear polarizability. In this situation we should use only the transverse part of macroscopic electromagnetic field as perturbative field. In the dipole approximation, the interaction with this field has the form

$$\hat{H}' = -\sum_n \hat{\boldsymbol{\mu}}_n \cdot \hat{\mathbf{E}}^{\perp}(\mathbf{n}), \tag{5.1}$$

where $\hat{\mathbf{E}}^{\perp}$ is a transverse part of the macroscopic field.

A four-wave mixing experiment may involve as many as three applied electric fields; the total field is given by

$$E^{\perp}(\mathbf{r},t) = \frac{1}{2}\sum_{j=1}^{3}\left[E_j^{\perp}\exp(i\mathbf{k}_j\cdot\mathbf{r}-i\omega_j t) + E_j^{*\perp}\exp(-i\mathbf{k}_j\cdot\mathbf{r}+i\omega_j t)\right], \tag{5.2}$$

where ω_j, $\mathbf{k}_j$, and $E_j^{\perp}$ is the frequency, wavevector and transverse electric field envelope of the j^{th} field, respectively. We shall consider only the *cw* case so that all $E_j^{\perp}$ are time independent. The third order monolayer polarization is given by

$$P(\mathbf{r},t) = \sum_{\kappa_s,\omega_s} \exp(i\kappa_s\cdot\mathbf{r}-\omega_s t)P(\kappa_s,\omega_s), \tag{5.3}$$

where $\mathbf{r}=m\mathbf{x}+n\mathbf{y}$, $\kappa_s = \pm\kappa_m \pm\kappa_n \pm\kappa_q$ and $\omega_s = \pm\omega_m \pm\omega_n \pm\omega_q$ with $m,n,q=1,2,\ldots$ and all combinations of plus and minus signs are allowed. κ_n is the tangential component of the n^{th} applied field wave vector $\mathbf{k}_n$ in the plane of the monolayer ($z=0$). Hereafter we choose the particular combination $\omega_s=\omega_1+\omega_2+\omega_3$ and $\kappa_s=\kappa_1+\kappa_2+\kappa_3$. Any other combination can be obtained by simply changing one or more κ_j to $-\kappa_j$, ω_j to $-\omega_j$ and $E_j^{\perp}$ to $E_j^{\perp *}$. The polarization per unit area is related to the applied electric fields via the third order susceptibility[27]

$$P(\kappa_s,\omega_s) = \chi^{(3)}(-\omega_s;\omega_1,\omega_2,\omega_3)E_1^{\perp}E_2^{\perp}E_3^{\perp}. \tag{5.4}$$

$\chi^{(3)}$ is the transverse third order nonlinear polarizability which gives the nonlinear polarization expressed through amplitudes of transverse electromagnetic fields. $\chi^{(3)}$ as defined in Eq. (5.4) can be used to calculate any four-wave mixing response. The role of scattering two exciton states (without binding) in $\chi^{(3)}$ was recently explored using Green function techniques, which resulted in mapping the problem onto coupled anharmonic oscillators.[15] A convenient technique for measuring the energies and lifetimes of the doubly excited states is two-photon absorption (TPA), which, is given by $\mathrm{Im}[\chi^{(3)}(-\omega;-\omega,\omega,\omega)]|E^{\perp}|^2$, where $E^{\perp}$ is the amplitude of the (single) external field. The complete expression for TPA includes two-photon transitions to the two-exciton continuum as well as to the biexciton states and is quite lengthy. The contribution of biexciton states to $\chi^{(3)}$ was obtained using the common sum over states expression for the nonliner response,[27,28] resulting in

$$\begin{aligned}\chi^{(3)}(-\omega;-\omega,\omega,\omega) = \frac{\mu^2\mu_{eb}^2(2\kappa)}{8\hbar^3a^2}\Bigg(&\frac{-1}{\omega-[E_b(2\kappa)-\omega(\kappa)]+i[\Gamma_b(2\kappa)+\gamma(\kappa)]/2}\,\frac{1}{i\gamma(\kappa)}\\ &\times\left\{\frac{1}{-\omega+\omega(\kappa)+i\gamma(\kappa)/2}+\frac{1}{\omega-\omega(\kappa)+i\gamma(\kappa)/2}\right\}\\ &-\left\{\frac{1}{\omega-[E_b(2\kappa)-\omega(\kappa)]+i[\Gamma_b(2\kappa)+\gamma(\kappa)]/2}-\frac{1}{\omega-\omega(\kappa)+i\gamma(\kappa)/2}\right\}\\ &\times\frac{1}{2\omega-E_b(2\kappa)+i\Gamma_b(2\kappa)/2}\cdot\frac{1}{\omega-\omega(\kappa)+i\gamma(\kappa)/2}\Bigg).\end{aligned} \tag{5.5}$$

These terms represent the four pathways in Liouville space[28] which contain the contribution of biexciton states to the two-photon absorption. In addition, we neglected small off-resonant terms (the rotating wave approximation). $\gamma(\kappa)$ and $\Gamma_b(2\kappa)$ are the decay rates of the exciton and biexciton states, which are introduced here phenomenologically.

The various terms in Eq. (5.5) can be combined to yield a more compact expression

$$\chi^{(3)}(-\omega;-\omega,\omega,\omega) = \frac{-\mu^2\mu_{eb}^2(2\kappa)}{4\hbar^3 a^2}\,\frac{\omega-\omega(\kappa)}{2\omega-E_b(2\kappa)+i\Gamma_b(2\kappa)/2} \times\left[\frac{1}{\omega-\omega(\kappa)+i\gamma(\kappa)/2}\right]^2 \times\frac{1}{-\omega+\omega(\kappa)+i\gamma(\kappa)/2}. \tag{5.6}$$

This form is naturally obtained from the nonlinear oscillator model of the medium.[15] Biexcitons may show up in TPA as new two-photon resonances at $2\omega = E_b(2\kappa)$, as given by the first denominator in Eq. (5.6). These resonances will be clearly visible and distinct from the single exciton resonance at $\omega = \omega(\kappa)$ provided the biexciton splitting is large compared with the damping

$$|E_b(2\kappa) - 2\omega(\kappa)| \gg \gamma(\kappa), \Gamma_b(2\kappa). \tag{5.7}$$

The biexciton resonances have a possible enhancement due to $\mu_{eb}^2(2\kappa)$ which, as discussed in Sec. IV, can be much larger than μ^2 for the H monolayer, but smaller than $4\mu^2$ for the J monolayer.

For the sake of clarity, in the expression for $\chi^{(3)}$ presented here, we have left out various geometric factors such as the polarization state of the external field (s or p) relative to the plane of incidence and the inner product between the field polarization vector (**e**) and the dipole moment vector (**m**). These factors are, of course, very important; the H monolayer, for example, cannot be excited by a field which is normally incident (k vector normal to the monolayer plane). For the J monolayer in this configuration, there is no problem and our expression for TPA can be used without modification, provided that e is parallel to $\boldsymbol{\mu}$. This condition can also be attained for an s polarized wave, at a nonzero incidence angle. To effectively excite the H monolayer requires a p polarized wave at a large incidence angle. The component of the external field tangent to the plane will not be absorbed, and therefore our TPA formula must be slightly modified. The positions of the TPA resonances and the oscillator strengths are, however, unaffected.

VI. CONCLUSION

In this paper, we have examined the possible formation of biexciton states in a monolayer of polar molecules, and calculated the two-photon absorption. Specific calculations were made for the case where the change in the permanent dipole moment of each molecule upon excitation from the ground to excited state is parallel to the transition dipole moment. The transition dipole moment was taken to be either parallel (J monolayer) or perpendicular (H monolayer) to the monolayer surface. For either configuration, a certain critical value of the interaction strength Θ is needed in order for a single bound state to emerge, and a second higher critical value is required for the existence of two bound states. In the optically important regime where $k \approx 0$, the critical values are $\Theta_1^J, \Theta_2^J = 1.6$, and 2.6 and $\Theta_1^H, \Theta_2^H = 1.1$ and 3.6. Using the definitions of Θ and the intermolecular couplings [Eqs. (4.1)–(4.4)], these translate into critical ratios of permanent dipole moment change to transition dipole moment $D \equiv \Delta\mu/\mu$, i.e., $D_1^J, D_2^J = 1.8$, and 2.3 and $D_1^H, D_2^H = 1.5$, and 2.7. Therefore, bound states can more easily be formed in H monolayers. In addition, the biexciton which first emerges is symmetric to the interchange of the x and y relative coordinates and is completely nodeless. The resulting large exciton–biexciton transition dipole moment leads to a strong two-photon absorption above the two-exciton continuum.

The position of the biexciton states depends primarily on the values μ and $\Delta\mu$. For example, for $\mu \cong \Delta\mu \cong 5$ D, the splitting of the biexciton state from the two-photon continuum may be order hundreds of cm^{-1} and in such situations should be detected experimentally. The possible observation of biexcitons depends crucially on the rate of bimolecular quenching. We need to identify conditions whereby the bimolecular quenching does not destroy the bound state of two-excitons so that biexcitons could be probed optically, e.g., by luminescence or nonlinear optical techniques. For biexciton states in semiconductors [Wannier–Mott excitons] the main decay channel is radiative, but in molecular crystals, the main channel should correspond to bimolecular annihilation. The reason is that exciton–exciton van der Waals interactions are weaker in semiconductors since the excitons have large radii and smaller transition dipoles. Biexciton states which are above the two-exciton continuum, will have an open decay channel which corresponds to a transition to the two-exciton continuum with the creation of optical or acoustical phonons. This channel, which is open even at low temperatures, provides a broadening mechanism for the biexciton states. The rate of bimolecular annihilation was previously calculated with the assumption that bimolecular quenching is weak,[23] in the sense that the corresponding width is small compared to the biexcitonic binding energy. In the future we hope to investigate this question for more general situations.

ACKNOWLEDGMENTS

The support of the National Science Foundation, the Science and Technology Center for photoinduced charge transfer, the U.S. Air Force Office of Scientific Research, and the Petroleum Research Fund, administered by the American Chemical Society, is gratefully acknowledged.

APPENDIX A

The molecular crystal Hamiltonian which includes exciton–exciton interactions was derived in Ref. 10 (see also Ref. 11).

Adopting a two-level model for each molecule (with a ground state 0 and an excited state f, with gas phase electronic transition energy $\Delta\epsilon_f$), the Hamiltonian is given by

$$\hat{H} = E_g + \hat{H}_1 + \hat{H}_2 + \hat{H}_3 + \hat{H}_4, \tag{A1}$$

where E_g is the ground state energy of the crystal, and

$$\hat{H}_1 = \sum_{nm}{}' \langle f0|\hat{V}_{nm}|00\rangle (b_{nf}^{\dagger} + b_{nf}), \tag{A2}$$

$$\hat{H}_2 = \sum_n (\omega_0 + \mathscr{D}_f) b^\dagger_{nf} b_{nf} + \sum_{n,m}{}' V^f_{nm} \left\{ b^\dagger_{mf} b_{nf} + \frac{1}{2} (b^\dagger_{nf} b^\dagger_{mf} + b_{nf} b_{mf}) \right\}, \tag{A3}$$

$$\hat{H}_3 = \sum_{n,m}{}' [\langle 0f | \hat{V}_{nm} | ff \rangle - \langle f0 | \hat{V}_{nm} | 00 \rangle] \times (b^\dagger_{nf} + b_{nf}) b^\dagger_{mf} b_{mf}, \tag{A4}$$

$$\hat{H}_4 = \sum_{n,m} A(n-m) b^\dagger_{nf} b_{nf} b^\dagger_{mf} b_{mf}, \tag{A5}$$

where

$$A(n-m) = \tfrac{1}{2} [\langle ff | \hat{V}_{nm} | ff \rangle + \langle 00 | \hat{V}_{nm} | 00 \rangle - 2 \langle f0 | \hat{V}_{nm} | f0 \rangle], \tag{A6}$$

$$\mathscr{D}_f = \sum_n \{ \langle 0f | \hat{V}_{nm} | 0f \rangle - \langle 00 | \hat{V}_{nm} | 00 \rangle \}, \tag{A7}$$

$$V^f_{nm} = \langle 0f | \hat{V}_{nm} | f0 \rangle. \tag{A8}$$

Here $b^\dagger_{nf}(b_{nf})$ is the creation (annihilation) operator for an excitation on the nth site. These operators satisfy the Pauli commutation relations. $\hat{V}_{nm}$ represents the intermolecular interaction and its matrix element is defined by

$$\langle \alpha\beta | \hat{V}_{nm} | \gamma\delta \rangle \equiv \int \varphi^\alpha_n \varphi^\beta_m \hat{V} \varphi^\gamma_n \varphi^\delta_m \, d\tau_n \, d\tau_m,$$

where φ^α_n represents the state where site n is in state α. The number operator for the excitations is

$$\hat{N} \equiv \sum_n b^\dagger_{nf} b_{nf}.$$

If we neglect in Eq. (1) the H_1 and H_3 terms, we obtain a zero order Hamiltonian which conserves the number of excitons (i.e., commutes with $\hat{N}$),

$$H_0 \equiv \epsilon_0 + \hat{H}_2 + \hat{H}_4. \tag{A9}$$

The last term in this Hamiltonian is responsible for the appearance of a bound two-exciton state (biexciton). In crystals made of the molecules with a center of inversion the interaction $A(n-m)$ vanishes in the dipole approximation, however, for nonsymmetrical crystals it follows from Eq. (A.6)

$$A(n-m) = \frac{1}{2} \Delta\mu_m \mathrm{T}_{mn} \Delta\mu_n, \tag{A10}$$

where

$$\Delta\mu_n = \langle f | \mu | f \rangle - \langle 0 | \mu | 0 \rangle \equiv \mu^f_n - \mu^g_n \tag{A11}$$

is the change in dipole moment upon optical excitation, and T_{nm} is the dipole–dipole electrostatic interaction tensor.

APPENDIX B: EVALUATION OF μ_{eb}(K) AND U_x(K)

In this Appendix, we derive Eqs. (4.10) and (4.11) for the exciton–biexciton transition dipole moment and biexciton normalization, respectively. We first write the summation over **r**, using Eq. (3.15), as

$$\sum_{\mathbf{r}}{}' \psi_K(\mathbf{r}) = \sum_{m,n}{}' G_{m\mathbf{x}+n\mathbf{y},\mathbf{x}} U_\mathbf{x}(\mathbf{K}) + G_{m\mathbf{x}+n\mathbf{y},\mathbf{y}} U_\mathbf{y}(\mathbf{K}), \tag{B1}$$

where the summation is taken over values of $\mathbf{r} = m\mathbf{x} + n\mathbf{y}$, excluding $-\mathbf{r}$ and **0**. Substituting in Eq. (B.1) for the Green function [Eq. (3.16)] and using $U_\mathbf{y}(\mathbf{K}) = R(\mathbf{K}) U_\mathbf{x}(\mathbf{K})$, where $R(\mathbf{K})$ from Eq. (3.10) is given by, $R(\mathbf{K}) \equiv [1 - M_{xx}(\mathbf{K})/M_{xy}(\mathbf{K})]$,

$$\sum_{\mathbf{r}}{}' \psi_\mathbf{K}(\mathbf{r}) = \frac{2U_x(\mathbf{K})}{N^2} \sum_{q_x,q_y} \frac{\Sigma'_{m,n} \cos[mq_xa + nq_ya]\cos[q_xa] + R(\mathbf{K})\cos[mq_xa + nq_ya]\cos[q_ya]}{E_b(\mathbf{K}) - \Omega(\mathbf{K},\mathbf{q})}. \tag{B2}$$

Now, if the sum in the numerator is denoted as x, then $y = 2x + (m = n = 0$ term) denotes the sum when the values of $-\mathbf{r}$ and **0** are included. Now the sum y is easily evaluated, $y = 2N^2 \delta_{q_x,0} \delta_{q_y,0} [\cos(q_xa) + R(\mathbf{K})\cos(q_ya)] + (m = n = 0$ term$) = 2[1 + R(\mathbf{K})] + (m = n = 0$ term). Substituting $x = (y-1)/2$ into Eq. (A.2) and letting N go to infinity, and further substituting this into Eq. (4.9) yields the exciton–biexciton transition dipole moment given by Eq. (4.9a).

In order to evaluate the normalization $U_x(\mathbf{K})$, we substitute Eq. (3.15) into the normalization condition

$$\sum_{\mathbf{r}}{}' |\psi_\mathbf{K}(\mathbf{r})|^2 = 1$$

giving

$$U^2_\mathbf{x}(\mathbf{K}) \sum_{m,n}{}' [G_{m\mathbf{x}+n\mathbf{y},\mathbf{x}} + R(\mathbf{K}) G_{m\mathbf{x}+n\mathbf{y},\mathbf{y}}]^2 = 1. \tag{B3}$$

The summation involves terms like

$$\frac{U^2_x(\mathbf{K})}{N^4} \sum_{q_x,q_y} \sum_{q'_x,q'_y} q'_x, q'_y \frac{\Sigma'_{m,n} (\cos[mq_xa + nq_ya])(\cos[mq'_xa + nq'_ya])\cos[q_xa]}{[E_b(\mathbf{K}) - \Omega(\mathbf{K},\mathbf{q})][E_b(\mathbf{K}) - \Omega(\mathbf{K},\mathbf{q}')]},$$

which are easily evaluated by the same summation technique used for the transition dipole moment. Collecting these various terms into Eq. (B.3) and solving for $U_x(\mathbf{K})$ yields Eq. (4.10).

---

[1] *Optical Nonlinearities and Instabilities in Semiconductors*, edited by H. Haug (Academic, New York, 1988).

[2] D. S. Chemla, D. A. B. Miller, P. W. Smith, A. C. Gossard, and W. Wiegmann, IEEE J. Quantum Electron. **20**, 265 (1984); S. Schmitt-Rink, D. A. B. Miller, and D. S. Chemla, Phys. Rev. B **35**, 8113 (1987); S. Schmitt-Rink, D. S. Chemla, and H. Haug, *ibid.* **37**, 941 (1988).

[3] M. L. Steigerwald and L. E. Brus, Acc. Chem. Res. **23**, 183 (1990); J. Warnock and D. D. Awschalom, Phys. Rev. B **32**, 5529 (1985).

[4] A. H. Hertz, Adv. Coll. Int. Sci. **8**, 237 (1977); B. Kopainsky and W. Kaiser, Chem. Phys. Lett. **88**, 357 (1982).

[5] S. DeBoer, K. J. Vink, and D. A. Wiersma, Chem. Phys. Lett. **137**, 99 (1987); S. DeBoer and D. A. Wiersma, Chem. Phys. Lett. **165**, 45 (1990).

[6] F. C. Spano, J. R. Kuklinski, and S. Mukamel, Phys. Rev. Lett. **65**, 211 (1990).

[7] D. Mobius and H. Kuhn, Isr. J. Chem. **18**, 375 (1979); J. Appl. Phys. **64**, 5138 (1988).

[8] D. S. Chemla and J. Zyss, *Nonlinear Optical Properties of Organic Molecules and Crystals*, (Academic, New York, 1987), Vols. I and II; *Langmuir–Blodgett Films*, edited by G. Roberts (Plenum, New York, 1990).

[9] F. F. So, S. R. Forrest, Y. Q. Shi, and W. H. Steier, Appl. Phys. Lett. **56**, 674 (1990).

[10] A. S. Davydov, *Theory of Molecular Excitons* (Plenum, New York, 1971).

[11] V. M. Agranovich, *The Theory of Excitons* (Nanka, Moscow, 1968) [in Russian].

[12] V. M. Agranovich, M. D. Galanin, *Electronic Exciton Energy Transfer in Condensed Matter* (North-Holland, Amsterdam, 1982).

[13] B. S. Toshich, Sov. Phys. Solid State **9**, 1346 (1967).

[14] D. Fox, Chem. Phys. **61**, 477 (1981); Mol. Cryst. Liq. Cryst. **57**, 39 (1980).

[15] (a) F. C. Spano and S. Mukamel, Phys. Rev. A **40**, 5783 (1989); **41**, 5243(E) (1990); (b) F. C. Spano and S. Mukamel, Phys. Rev. Lett. **66**, 1197 (1991).

[16] H. Ishihara and K. Cho, Phys. Rev. B **42**, 1724 (1990).

[17] V. M. Agranovich, Sov. Phys. Solid State **12**, 430 (1970); V. M. Agranovich, *Spectroscopy and Dynamics of Excitons in Molecular Systems*, edited by V. M. Agranovich and R. Hochstrasser, (North-Holland, Amsterdam, 1983) p. 83; V. M. Agranovich, N. A. Efremov, and E. P. Kaminskaya, Opt. Commun. **3**, 387 (1971).

[18] N. A. Efremov and E. P. Kaminskaya, Sov. Phys. Solid State **14**, 1012 (1972).

[19] N. A. Efremov and M. A. Kozhushner, Sov. Phys. Solid State **13**, 2993 (1972); N. A. Efremov and E. P. Kaminskaya, Sov. Phys. Solid State **15**, 2221 (1974).

[20] V. M. Agranovich and O. A. Dubovskii, JETP Lett. **3**, 223 (1966).

[21] M. R. Philpott and P. G. Sherman, Phys. Rev. B **12**, 5381 (1975).

[22] M. Orrit and P. Kottis, Adv. Chem. Phys. **74**, 1 (1988).

[23] V. M. Agranovich and S. Mukamel, Phys. Lett. A **147**, 155 (1990).

[24] M. Wortis, *Phys. Rev.* **132**, 85 (1963); N. Fukuda and M. Wortis, J. Phys. Chem. Solids **24**, 1675 (1963).

[25] V. M. Agranovich and V. L. Ginzburg, *Spatial Dispersion in Crystal Optics and Excitons* (Springer, Berlin, 1984).

[26] S. I. Pekar, *Crystal Optics and Additional Light Waves*, (Benjamin, Reading, 1983).

[27] N. Bloembergen, *Nonlinear Optics* (Benjamin, New York 1985).

[28] S. Mukamel and R. F. Loring, J. Opt. Soc. Am B **3**, 595 (1986).